NANO LETTERS

Mechanism of Exfoliation and Prediction of Materials Properties of Clay−Polymer Nanocomposites from Multiscale Modeling

James L. Suter, Derek Groen,[†] and Peter V. Coveney[*]

Centre for Computational Science, University College London, 20 Gordon Street, London, WC1H 0AJ, United Kingdom

S Supporting Information

ABSTRACT: We describe the mechanism that leads to full exfoliation and dispersion of organophilic clays when mixed with molten hydrophilic polymers. This process is of fundamental importance for the production of clay−polymer nanocomposites with enhanced materials properties. The chemically specific nature of our multiscale approach allows us to probe how chemistry, in combination with processing conditions, produces such materials properties at the mesoscale and beyond. In general agreement with experimental observations, we find that a higher grafting density of charged quaternary ammonium surfactant ions promotes exfoliation, by a mechanism whereby the clay sheets slide transversally over one another. We can determine the elastic properties of these nanocomposites; exfoliated and partially exfoliated morphologies lead to substantial enhancement of the Young's modulus, as found experimentally.

KEYWORDS: Multiscale modeling, clay−polymer nanocomposites, exfoliation dynamics, materials properties
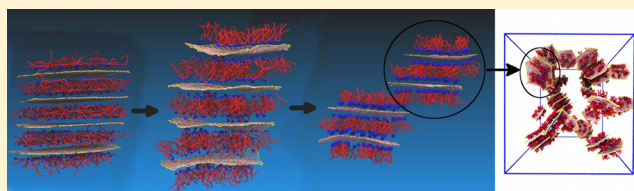
The search for new materials with specified performance properties continues apace. The incentives come not only from curiosity driven research but also from the pressure to meet important economic and societal needs. However, the history of innovation in materials design, and the path from initial discovery to implementation in engineering and manufacturing contexts, is a fraught one. Innovations frequently take decades to make their way into commercially viable applications. One of the central reasons for such problems stems from the difficulty of moving between the promise held out at the small ("microscopic") scale by the entity discovered and the behavior of such substances on larger scales appropriate to their use in various applications. This has led to a vast amount of larger scale engineering and manufacturing research and development, almost all of which is conducted experimentally in a largely trial and error fashion. Here we describe a complementary approach, one based on a virtual materials modeling laboratory. Rather than simply synthesizing a great many samples of a material and testing these, we aim to predict materials properties from "first-principles", that is, based on the fundamental description of the starting ingredients in terms of their atomic and molecular composition and structure and the processing conditions.

This is possible through a multiscale scheme that links these very short length (and time) scale descriptions to the larger ones that inform materials properties. We show how our scheme, thus far developed for the study of nanocomposite materials, can be successfully applied to understand and predict the behavior of exfoliating clay−polymer nanocomposites. Within four years of their initial discovery, Toyota was making car components from composites comprised of clay and nylon. However, since that early work, and notwithstanding a vast

literature on the subject, the field has failed to live up to expectations.[1] There remains a very poor level of understanding of the mechanism of action of these materials, and no control over the outcome of mixing arbitrary polymers with clays.[2,3] Models are therefore required to understand how large-scale dispersion of clay layers in polymers can be achieved and to determine structure−property relationships, thereby enabling the design of materials with desired properties. In this paper, we provide a clear and detailed, chemically specific, explanation for the mechanism of exfoliation of clays by suitable polymers and why, following the dispersion of the individual clay platelets, the resultant materials exhibit very favorable materials properties.

Our multiscale scheme uses short time scale atomistic simulations to create interaction parameters for coarse-grained (CG) particles that represent several atoms.[4−6] For clay polymer composites, we require a substantial number of atomistic simulations to define all interaction potentials. These simulations include matching to structural parameters using Iterative Boltzmann Inversion[5,7] and to free-energy profiles for highly interacting CG particles[8] to build up a complete set of chemically specific CG potentials in the vicinity of clay interfaces. For more details, see Supporting Information. This degree of coarse-graining produces speed-ups of order of 100 times, while retaining molecular specificity,[9] allowing us to reach length and time scales approaching a hundred nanometers and microseconds, respectively. Almost all atomistic studies of clay−polymer nanocomposites have focused only on the interlayer region between the clay layers, effectively simulating

an infinite clay mineral system; such simulations give information on the interfacial behavior at the basal surface but do not describe the large-scale behavior (i.e., dispersion, aggregation) of clay layers.[10,11] Simulations without molecular detail, such as self-consistent phase field theory, provide predictions about the thermodynamic tendency for clay layers to exfoliate based on a mean field approximation[12−17] but, again, they cannot describe the chemically specific nature of the clays and polymers.[18] For a comprehensive review of multiscale modeling of polymer nanocomposites, see Zeng et al.[19]

In a significant advance on our previous multiscale modeling of pristine clays with hydrophilic polymers, which led to intercalated clay−polymer systems,[4] in this study we examine the process of clay layer exfoliation using similar methods.

To do so, we have chosen a clay, surfactant, and polymer combination that is known to produce at least partially exfoliated clay layers: montmorillonite clay, a quaternary ammonium dimethyldioctadecylammonium ionic surfactant, which has two alkyl chains (each of length C_{18}), and hydrophilic poly(ethylene)-glycol (PEG) as the polymer matrix (Figure 1).[20−23] This combination has been shown exper-
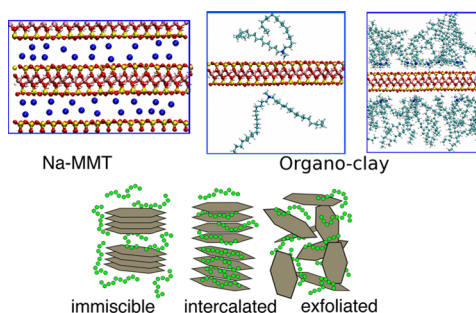

Figure 1. Top left: Na-montmorillonite is a layered mineral consisting of octahedrally coordinated aluminum oxide between two silica tetrahedral layers (the atoms are colored as followed: Al = pink, Ai = yellow, O = red, H = white, Na = blue, C = Cyan). Top right: exchanging the alkali ions in the interlayer for quaternary ammonium ions expands the clay interlayer spacing and gives the clay a hydrophobic character. Bottom: The clay layers can either remain aggregated (immiscible), or can penetrate the clay interlayer (intercalated), or the clay layers can fully disperse (exfoliated).

imentally to produce exfoliated clay layers, as demonstrated by the lack of peaks in X-ray diffractograms following melt intercalation.[24] Although PEG-clay nanocomposites are often prepared using solution methods, melt processing is a more industrially convenient route of preparation; our simulations therefore take place at elevated temperatures and pressures (500 K and 300 atm) in the absence of water.

We have simulated three models of differing clay surface charge density (through isomorphic substitution) and hence surface density of quaternary ammonium surfactants. Each model is comprised of 8 tactoids with each tactoid composed of 4 layers (32 layers in total). Each clay layer is of hexagonal shape with a diameter of approximately 100 Å; in total, they

comprise approximately 2−6% of the volume of the simulation cell, depending on whether we use the thickness of the clay sheet (1 nm) or the initial separation between clay layers (20−28 Å) as the thickness of the platelets. The models are listed in Table 1. Each clay layer possesses an aspect ratio of approximately 10.

Montmorillonite clays are often quoted as having an aspect ratio of between 10 and 1000;[25] our models are therefore at the lower end of this distribution. Atomic force microscopy and photocorrelation spectroscopy studies indicated that the sizes of Na-montmorillonite clay exhibited a bimodal distribution with wide size distributions.[26] The average dimensions of the first population were typically 320−400 nm long/250 nm wide and 200−250 nm long/120 nm wide for natural and synthetic clays, respectively. The population with smaller sizes were, on average, 65 and 50 nm long and 35 and 25 nm wide for natural and synthetic clays, respectively. This is of the same order of magnitude as the lateral dimensions of the clay platelets in our simulations (10 nm), giving us confidence that our models are representative of clay layers found experimentally.

With an aspect ratio of 10 for our models, the basal clay interactions will dominate, as will be the case for clays with higher aspect ratios. Thus, the results we report should also be applicable to much larger clays, such as those seen in the larger size distribution by Cadene et al.[26]

Initially, the tactoids are in their aggregated state with no polymer in the interlayer gallery. We vary the density from a very low charge montmorillonite clay (5% of Al^{3+} substituted with Mg^{2+}, referred to as **I** in the remainder of this paper), via a typical Wyoming montmorillonite (11%, referred to as **II**) to a high charge density clay (17% substitution rate, referred to as **III**). These correspond to an approximate cation exchange capacity (CEC) of 0.31 (0.28 including clay edges) meq/g, 0.69 (0.62 including clay edges) meq/g, and 1.05 (0.98 including clay edges) meq/g, respectively.

Our models were created by constructing a clay tactoid comprising four hexagonal layers, each composed of (110), (010), and (001) surfaces, with lateral dimensions measuring approximately 98 Å by 104 Å. Surfactant molecules were then added to this four clay-layer tactoid at the atomistic level, and subsequently relaxed using atomistic molecular dynamics at 500 K, leading to the initial d-spacings listed in Table 1. The partial charges on the edges of the clay sheet were determined through quantum mechanical simulations.[27] This tactoid was subsequently coarse-grained, and 100 monomer PEG polymers, corresponding to a molecular weight of 4372 g mol^{-1}, were built according to the protocol described by Suter et al.[4] The simulations are replicated in a 2 × 2 × 2 array to form an 8 tactoid (32 clay layers) initial model (see Table 1). All simulations were performed at 500 K and at relatively high pressure (300 atm). The lattice parameters were allowed to vary under constant pressure and temperature conditions (NPT) for the first 100 ps, after which each simulation was run with constant volume (NVT). The simulations were performed using the LAMMPS molecular dynamics code,[28,29] using a time

Table 1. Organo-Modified Clay: PEG Models Studied in This Paper

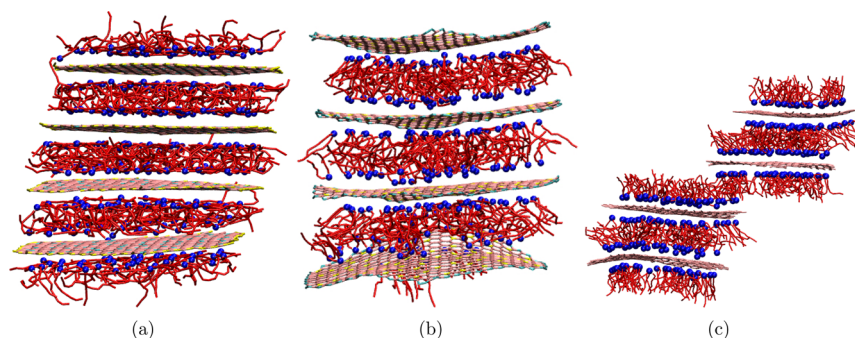| system	substitution rate	simulation cell dimensions (Å)³	num. of CG atoms/all atoms equivalent	initial/intercalated d-spacing Å
I	5%	407 × 440 × 448	671200/4870912	20 Å/15−20 Å
II	11%	415 × 415 × 449	667904/4829856	25 Å/32 Å
III	17%	504 × 504 × 602	1363264/9568096	28 Å/32 Å

Figure 2. Snapshots from CG molecular dynamics simulations of a selected alkyl ammonium treated clay tactoid immersed in a melt of PEG polymer. (CG clay surface = pink, charge sites = green, edge sites = yellow, surfactant ammonium group = blue, alkyl chains = red.) The PEG polymers have been removed to aid visualization. (a) We show the organoclay model before interaction with the PEG polymer for model **II**. In (b), the PEG polymer has intercalated into the clay galleries and the separation between the clay layers has increased. In (c), we observe the uppermost two clay layers diffusing away from each other, eventually forming an exfoliated morphology, achieved by the upper clay layers translating in the plane of the clay tactoid layers.
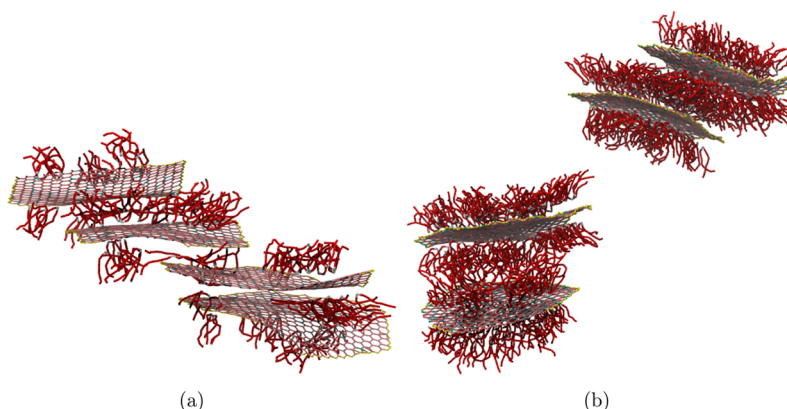

Figure 3. Snapshots from subdomains of simulations for (a) model **I** and (b) **III** after approximately 0.2 μs. We see that for the low charge system (a), the clay tactoid stack forms a tilted configuration with a large number of alkyl ammonium chains interacting with the bulk PEG polymer (not shown). This configuration appears to be stable on the time scale of our simulations. (b) For model **III**, the clay layers have already separated and ultimately become fully exfoliated (see Figure 4c).

step of 2 fs. To facilitate our simulations, we used our python-based toolkit, FabMD.[30] Each simulation was run for >2 μs. Further computational details, including the procedure for generating the materials properties, are listed in the Supporting Information.

In all the models listed in Table 1, we observe an initial expansion as the polymer intercalates between the clay layers over a short time period (approximately 2 ns). The intercalated *d*-spacings are shown in Table 1. Snapshots of this process are shown in Figure 2 for model **II**. The PEG polymer molecules intercalate into the gallery predominately adjacent to the clay surface, illustrating the favorable interactions between the hydrophilic PEG polymer molecules and the surface as compared to that of the alkyl chains. The rapid dynamics of polymer intercalation has been previously observed experimentally by Vaia and Giannelis and is attributed to the unhindered nature of the confined polymers (there are fewer entanglements, unlike in the bulk).[31]

The separation between the clay layers increases by approximately 7 Å. This is consistent with an extra layer of PEG molecules resident on each clay surface. In Supporting Information Figure SI.20, we plot the density profile perpendicular to the clay surface for species within the clay interlayer, which confirms that the majority of the PEG molecules reside on the clay surfaces while the alkyl chains of

the surfactant cation extend perpendicular to the clay layers accompanied by clay layer expansion. Once the monolayer of PEG molecules on the clay surface is filled, no further expansion occurs. We can infer that at this point the enthalpic interactions between the polymer and the clay are no longer enough to overcome the entropy loss through polymer confinement.[12] There is no further driving force for the clay layers to expand. The low density of PEG polymer molecules in the center of the interlayer confirms that the interaction of the PEG polymer with the nonpolar alkyl chains of the surfactant is unfavorable, again lowering the tendency for further PEG polymer intercalation.

For models **II** and **III**, once the fast intercalation of PEG molecules has occurred we observe on longer time scales (>500 ns) the diffusion of the clay layers away from the clay platelets to form exfoliated morphologies. We show this mechanism in Figure 2 for model **II** and Figure 3 for model **III**. After more than 3 μs of simulation time, the structures of our eight tactoid models are shown for models **I**, **II**, and **III** in Figure 4. We see that for model **II** there is a mixture of partially and totally exfoliated clay layers while, and for model **III** all the clay tactoids have exfoliated into single dispersed layers.

We find that the mechanism for the exfoliation of the clay layers does not involve the clay layers expanding perpendicular to the clay surface but rather involves the layers translating
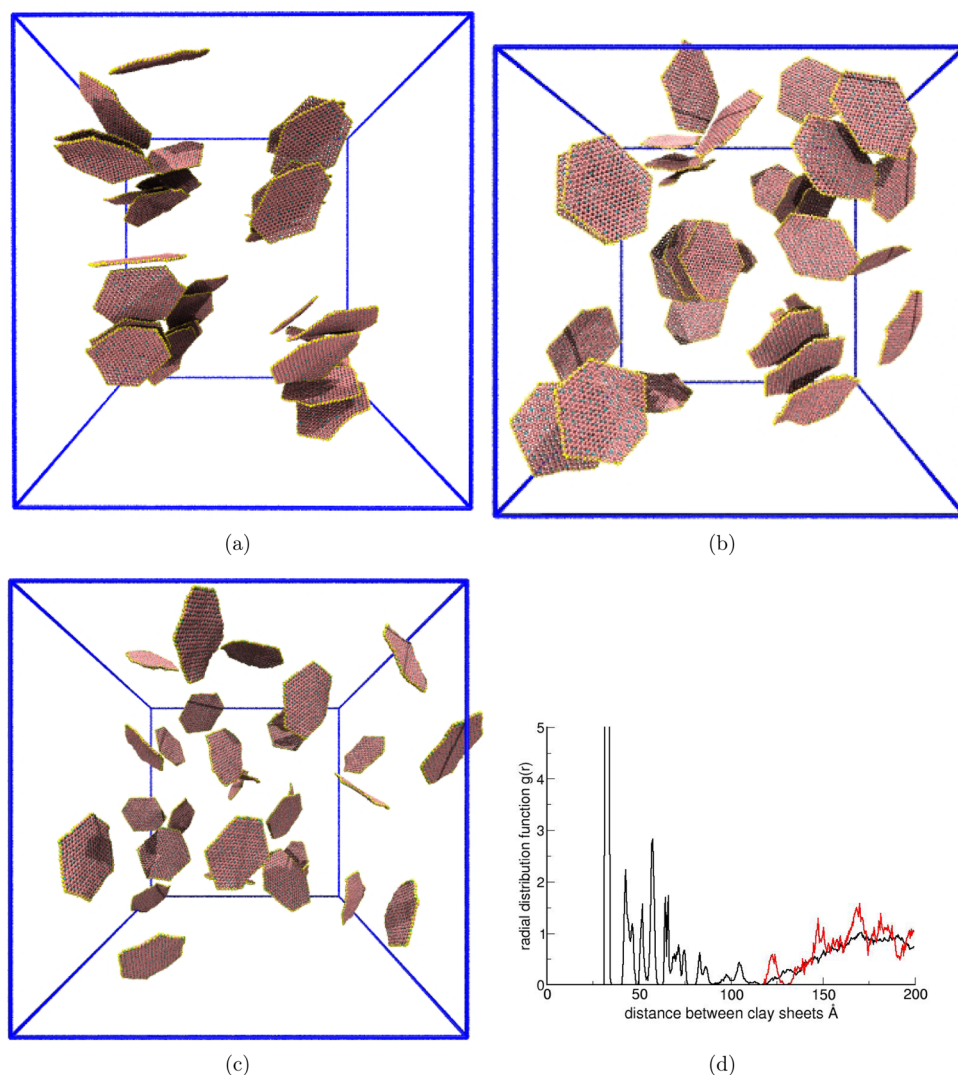
Figure 4. Snapshots from the CG molecular dynamics simulation, containing 8 tactoids (32 layers) of models (a) **I**, (b) **II**, and (c) **III** after approximately 3 μs of simulation. The PEG polymer and surfactant molecules have been removed to aid visualization. (d) The radial distribution function for the center-of-mass of the clay layers for model **II** (black) and model **III** (red) averaged over the last 10 ns of simulation, illustrating that model **III** is fully dispersed.

parallel to one another, as illustrated in Figure 3. For model **II**, we observe this occurring randomly for different interlayers within the tactoid; for example, in Figure 2 the inner-interlayer exhibits this translational motion, while in other tactoids one of the outer layers undergoes lateral motion and diffuses away.

The incomplete exfoliation of clay layers in model **II** may be in part due to different sections of the same polymer molecule initially intercalating into either adjacent clay interlayers or bridging between clay layers within the same interlayer.[4] Where various parts of a single PEG molecule are adsorbed on different clay surfaces, including different interlayers, this serves to resist any translational diffusion of the clay layers (see Figure 5). As a result, for model **II** we see a distribution of exfoliated and partially exfoliated clay platelets. With much larger platelets, it could be envisaged that the greater number of bridging configurations within the interlayers would resulting in full exfoliation becoming a slower process, leading to a greater number of partially exfoliated platelets. However, for model **III**, as Supporting Information Figure SI.15 demonstrates, there is much less PEG molecule density in the center of the interlayer, indicating that there are fewer PEG molecules bridging the
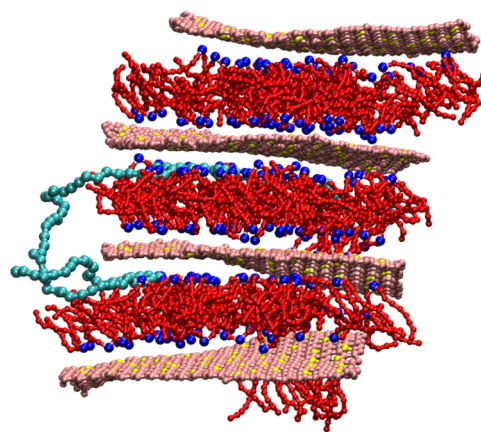

Figure 5. An illustration of a PEG polymer (cyan) adsorbed within two different clay layers in adjacent clay interlayers in model **II**. Such configurations are likely to inhibit the diffusive process leading to clay layer exfoliation.

interlayer. This is likely to be due to the combination of a greater number of ammonium groups on the clay surface (restricting the surface area available to the PEG molecules) and the greater initial *d*-spacing. As a result, there is no attraction between the clay layers and they exfoliate rapidly.

Experimentally, we can compare our structural observations with commercially available Cloisite 20A, an organically modified montmorillonite clay with dimethyl dihydrogenated tallow quaternary ammonium surfactants (alkyl chain lengths between C_{14} and C_{18}) and a CEC of 0.95. In the work of Loyens et al.,[24] when Cloisite 20A was blended with PEG using melt extrusion, a variety of nanostructures were found, depending on polymer molar mass and clay volume fraction: lower molecular mass PEG (100 000 g mol^{-1}) at 5% clay vol. and small clay volume fractions produced a peak in the small-angle X-ray scattering measurements (SAXS) diffraction spectra at 37 Å as well as at higher spacings. The 32 Å *d*-spacing we have calculated via multiscale modeling for the intercalated structures is therefore in good agreement with experimental observations. In general, intercalation of PEG with molecular weight in the range 10^5–10^6 g mol^{-1} in organically modified clay composites results in reported *d*-spacings in the range of 34 ± 4 Å.[32−36] Higher molecular weight PEGs were shown to produce exfoliated morphologies (no peaks in the SAXS diffraction spectra);[24] we can assume, therefore, that in the lower molecular weight PEG models a combination of exfoliated and intercalated morphologies are present. The Cloisite 15A system is a similarly organically modified montmorillonite clay but has a higher CEC of 1.25; this provides a comparison with model **III**. Although no melt processing has been reported in the literature with PEG polymer, Hyun et al. found that using the solvent casting method the Cloisite 15A nanocomposite showed better dispersion via transmission electron microscopy (TEM) and steady shear viscosity measurements, compared with the Cloisite 20A clay system.[33]

In Figure 6 we show the stress−strain behavior for models **II** and **III**, calculated at 100 K, using a strain rate of 1×10^{-8} s. The final snapshots of our simulations were rapidly cooled from 500 to 100 K over 4 ns to produce a quenched amorphous system in its glassy state from which stress−strain curves were computed. We have estimated the glass transition temperature
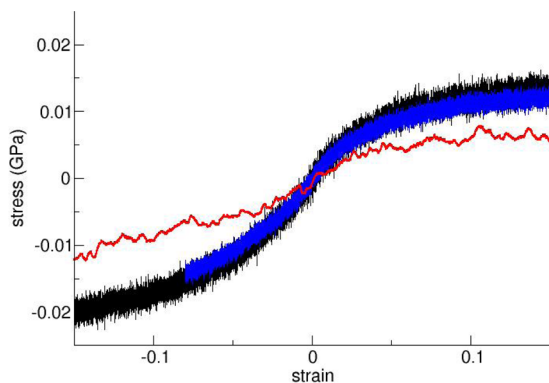
(T_g) from the change in the slope of the volume versus temperature curve (see Supporting Information) to be approximately 220 K. We wish to examine the elastic properties in the glassy state of the composite; hence, we have chosen a temperature well below T_g such that we can determine the stiffness, as at this temperature the system will remain in a glassy state when strained. There is no evidence that crystallization of the PEG molecules is occurring (see Supporting Information for more details); we can be sure that we are observing the response of the quenched amorphous system. We find that the stress−strain curve for partially exfoliated model **II** and totally exfoliated model **III** are almost identical, even though model **III** has a smaller clay volume fraction. We find Young's moduli of 0.284 GPa ± 0.001 and 0.266 GPa ± 0.001, respectively; this is over twice that of the neat polymer (0.126 GPa). Our previous models of non-intercalated clay tactoids with a pristine montmorillonite clay immersed in PEG polymer produced a Young's modulus of 0.137 GPa.[4] Note that the calculations reported for the studies at 100 K are not expected to be quantitatively correct, as they employ potential parametrizations obtained at higher temperatures. However, the qualitative trends are expected to remain intact, as previously found, for example, when examining the Young's modulus of polystyrene−silica composites.[37]

We observe that exfoliated morphologies significantly enhance the elastic properties of the composite and that even partially exfoliated clay morphologies provide a large enhancement. Ratna et al. reported a similar increase in Young's modulus for PEG−clay nanocomposites formed through solution casting, which increased from approximately 0.1 GPa for pure PEG to 0.14 GPa for composites containing 2.5% clay and to 0.25 GPa for those containing 5% clay.[34] The absolute values, although reasonably close, can not be compared due to the qualitative nature of the CG potentials at 100 K and the solution casting method used experimentally. The enhancement of the Young's modulus of a factor of approximately 2 compared to the bulk polymer is also comparable to a 1.74 factor for the longitudinal stiffness, E_{11}, for composites filled with unidirectional disklike particles using the Halpin−Tsai micromechanical model[38] (see Supporting Information for details).

To summarize, we have shown how organically treated clays promote exfoliation and report the first ever multiscale modeling and simulation study that captures the full process, from the melt intercalation of suitable polymers into such organophilic clays, to the dispersion of individual clay platelets within the polymer matrix. At such longer time scales, we can compute the materials properties of the resultant nano-composite and find that it exhibits substantially enhanced mechanical properties compared to the properties of its component parts. The predictions of our models are in generally good agreement with experimental observations. In the future, we will investigate the role of processing on materials properties, such as shearing and extensional flow, which are of particular importance in the context of hydrophobic polymers, for example, polystyrene.[39] Moreover, our multiscale methods are at a very early stage of development and many improvements to their quantitative capabilities can be expected in the future, as well as their transferability between different thermodynamic states. We anticipate that with forthcoming progress in both experimental observations and computational methods the latter will evolve into a powerful tool that will be able to guide materials property prediction

Figure 6. Stress−strain curves for uniaxial compression and extension of our organoclay models **II** (black) and **III** (blue). The neat PEG polymer stress−strain curve is also shown (red). We calculate elastic properties (the Young's modulus) from the gradient of the stress−strain curve. The starting configurations for these simulations are the final simulation snapshots shown in Figure 4, cooled down to 100 K.

based on the chemical specificity of the ingredients and their processing conditions.

■ ASSOCIATED CONTENT

Ⓢ Supporting Information

■ AUTHOR INFORMATION

Corresponding Author

*E-mail: p.v.coveney@ucl.ac.uk.

Present Address

†Department of Computer Science, Brunel University London, Uxbridge, Middlesex, UB8 3PH, United Kingdom

Notes

The authors declare no competing financial interest.

■ ACKNOWLEDGMENTS

■ REFERENCES

(1) Okada, A.; Usuki, A. *Macromol. Mater. Eng.* **2006**, *291*, 1449–1476.

(2) Chen, B.; Evans, J. R. G.; Greenwell, H. C.; Boulet, P.; Coveney, P. V.; Bowden, A. A.; Whiting, A. *Chem. Soc. Rev.* **2008**, *37*, 568–594.

(3) Ray, S. S. *Macromol. Chem. Phys.* **2014**, *215*, 1162–1179.

(4) Suter, J. L.; Groen, D.; Coveney, P. V. *Adv. Mater.* **2015**, *27*, 966–984.

(5) Ruehle, V.; Junghans, C.; Lukyanov, A.; Kremer, K.; Andrienko, D. *J. Chem. Theory Comput.* **2009**, *5*, 3211–3223.

(6) Karabasov, S.; Nerukh, D.; Hoekstra, A. G.; Chopard, B.; Coveney, P. V. *Philos. Trans. R. Soc., A* **2014**, *372*, 20130390.

(7) Müller-Plathe, F. *ChemPhysChem* **2002**, *3*, 754–769.

(8) Roux, B. *Comput. Phys. Commun.* **1995**, *91*, 275–282.

(9) Johnston, K.; Harmandaris, V. *Soft Matter* **2013**, *9*, 6696–6710.

(10) Cygan, R. T.; Greathouse, J. A.; Heinz, H.; Kalinichev, A. G. *J. Mater. Chem.* **2009**, *19*, 2470–2481.

(11) Greathouse, J. A.; Johnson, K. L.; Greenwell, H. C. *Minerals* **2014**, *4*, 519–540.

(12) Vaia, R. A.; Giannelis, E. P. *Macromolecules* **1997**, *30*, 7990–7999.

(13) Balazs, A. C.; Singh, C.; Zhulina, E. *Macromolecules* **1998**, *31*, 8370–8381.

(14) Buxton, G. A.; Balazs, A. C. *J. Chem. Phys.* **2002**, *117*, 7649–7658.

(15) Balazs, A. C.; Bicerano, J.; Ginzburg, V. V. In *Polyolefin Composites*; Nwabunma, D., Kyu, T., Eds.; John Wiley & Sons, Inc.: Hoboken, NJ, 2008; pp 415–448.

(16) Ginzburg, V. V.; Balazs, A. C. *Macromolecules* **1999**, *32*, 5681–5688.

(17) Ginzburg, V. V.; Singh, C.; Balazs, A. C. *Macromolecules* **2000**, *33*, 1089–1099.

(18) Ginzburg, V. V.; Weinhold, J. D.; Jog, P. K.; Srivastava, R. *Macromolecules* **2009**, *42*, 9089–9095.

(19) Zeng, Q.; Yu, A.; Lu, G. *Prog. Polym. Sci.* **2008**, *33*, 191–269.

(20) Heinz, H.; Koerner, H.; Anderson, K. L.; Vaia, R. A.; Farmer, B. L. *Chem. Mater.* **2005**, *17*, 5658–5669.

(21) Fu, Y.-T.; Heinz, H. *Chem. Mater.* **2010**, *22*, 1595–1605.

(22) Liu, X.; Lu, X.; Wang, R.; Zhou, H.; Xu, S. *Clays Clay Miner.* **2007**, *55*, 554–564.

(23) Losego, M. D.; Blitz, I. P.; Vaia, R. A.; Cahill, D. G.; Braun, P. V. *Nano Lett.* **2013**, *13*, 2215–2219.

(24) Loyens, W.; Jannasch, P.; Maurer, F. H. *Polymer* **2005**, *46*, 903–914.

(25) Ray, S. S.; Okamoto, K.; Okamoto, M. *J. Appl. Polym. Sci.* **2006**, *102*, 777–785.

(26) Cadene, A.; Durand-Vidal, S.; Turq, P.; Brendle, J. *J. Colloid Interface Sci.* **2005**, *285*, 719–730.

(27) Suter, J. L.; Kabalan, L.; Khader, M.; Coveney, P. V. *Geochim. Cosmochim. Acta* **2015**, *169*, 17–29.

(28) Plimpton, S. Large-scale atomic/molecular massively parallel simulator. http://lammps.sandia.gov (accessed Nov. 18, 2015)

(29) Plimpton, S. J. *J. Comput. Phys.* **1995**, *117*, 1–19.

(30) Groen, D.; Bhati, A.; Suter, J. L.; Hetherington, J.; Zasada, S. J.; Coveney, P. V. FabMD. https://github.com/UCL-CCS/FabSim, 2015 (accessed Nov. 18, 2015).

(31) Krishnamoorti, R.; Vaia, R. A.; Giannelis, E. P. *Chem. Mater.* **1996**, *8*, 1728–1734.

(32) Kelarakis, A.; Giannelis, E. P. *Polymer* **2011**, *52*, 2221–2227.

(33) Hyun, Y. H.; Lim, S. T.; Choi, H. J.; Jhon, M. S. *Macromolecules* **2001**, *34*, 8084–8093.

(34) Ratna, D.; Divekar, S.; Samui, A.; Chakraborty, B.; Banthia, A. *Polymer* **2006**, *47*, 4068–4074.

(35) Choi, H. J.; Kim, S. G.; Hyun, Y. H.; Jhon, M. S. *Macromol. Rapid Commun.* **2001**, *22*, 320–325.

(36) Lim, S.; Kim, J.; Chin, I.; Kwon, Y.; Choi, H. *Chem. Mater.* **2002**, *14*, 1989–1994.

(37) Rahimi, M.; Iriarte-Carretero, I.; Ghanbari, A.; Böhm, M. C.; Müller-Plathe, F. *Nanotechnology* **2012**, *23*, 305702.

(38) Sheng, N.; Boyce, M. C.; Parks, D. M.; Rutledge, G.; Abes, J.; Cohen, R. *Polymer* **2004**, *45*, 487–506.

(39) Bujdak, J. *J. Phys. Chem. C* **2015**, *119*, 12016–12022.